DOI: 10.1002/chem.201100081

Confined Metallophilicity within a Coordination Prism

Guo-Fen Gao, Mian Li, Shun-Ze Zhan, Zhi Lv, Guang-hui Chen, and Dan Li*[a]

Metallophilicity (also called metal–metal bonding) is a structural chemical concept that describes unusual chemical bonding between closed-shell metal centers, despite the formal nd^{10} electronic configurations.[1,2] During the past decades, the occurrence of metal–metal interactions have been testified by compelling experimental evidence,[2,3] but the origin remains controversial.[4–6] Hoffmann and co-worker postulated that the hybridization of *n*d orbitals with $(n+1)$s and $(n+1)$p orbitals is responsible for the metal–metal bonding;[4] this was strongly supported by the direct observation of d orbital holes in Cu_2O.[3] However, higher-level calculations performed by Pyykkö et al. concluded that metallophilic attraction does not involve electronic transition, but is just another van der Waals force based on correlation and relativistic effects.[5] Cotton and co-workers also claimed that their DFT calculations did not reveal any evidence for possible metal–metal bonding, despite very short Cu^I–Cu^I distances; hence contradicting the above-mentioned hybridization hypothesis.[6]

The phenomenon of metallophilicity is usually encountered in coinage metal (Cu^I, Ag^I, and Au^I) compounds,[2] which include a classic family of cyclic, trinuclear, Cu^I-pyrazolate complexes[7–10] (henceforth referred to as Cu_3, see Figure 1) assembled through Cu^I–Cu^I interactions. Recently, such coinage-metal (Cu^I and Ag^I)-pyrazolate trimers were used by us[11] and others[12] as building blocks to assemble intriguing, supramolecular architectures. Note, in both oligomeric[7–10] and polymeric[11,12] Cu_3-based aggregates, the intertrimeric Cu^I–Cu^I contact, rather than the intratrimeric one, functions as bright phosphor and features interesting luminescent behaviors[7–9] triggered by the unassisted dimer of trimers (henceforth referred to as Cu_6, see Figure 1). Herein, we describe the design and synthesis of a new coordination prism, namely, $[Cu_6L_3]$ (L = *p*-xylylene-bis(3,5-dimethyl)pyrazol-4-yl), exhibiting an unprecedented Cu_6 stacking mode, with which we are able to capture structural and spectroscopic evidence of enhanced metallophilicity. Furthermore, upon DFT analysis, an unusual situation of grand orbital hybridization at the excited state of the coordination prism is unveiled.

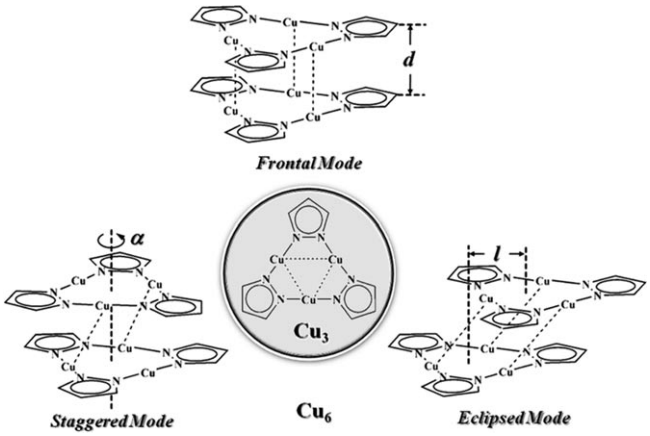

Figure 1. Molecular diagram of the Cu_3 trimer and the possible Cu_6 dimer of trimers. There are three related stacking modes of Cu_6 defined by a set of geometrical parameters (*d*, *l*, and α). Assuming each Cu_3 triangle defines a plane and a centroid, the perpendicular separation of the two Cu_3 planes is set as the first parameter, *d*. If the centroid distance, which is the smallest value, equals the value of *d*, and the orthogonal projections of the two Cu_3 triangles coincide with each other, the stacking arrangement is called a frontal mode. The eclipsed mode refers to the situation when the two parallel Cu_3 triangles show horizontal displacement, where the horizontal distance of the two centroids is set as the second parameter, *l*. The introduction of the third parameter, α, which describes the rotational angle when the orthogonal projections of the two Cu_3 triangles do not coincide, generates the staggered mode when $\alpha = 60°$.

Interestingly, all reported Cu_6 cases, including theoretical optimization[10] and experimental observation,[7–9,11] are found in the staggered mode (Figure 1) or in a combination of the eclipsed and staggered modes (usually called chair conformation)—no Cu_6 frontal mode has been documented so far, due to energetic and steric effects. Our presynthetic consideration for targeting the frontal mode involved the designer ligand L with bispyrazolate components for construction of Cu_3 units, two of which that were supposed to be fixed in a parallel fashion by three semirigid xylylene linkers with appropriate binding angles to yield a cage-shaped Cu^I-pyrazolate molecule with a prism conformation.

As shown in Figure 2, the crystal structure of the $[Cu_6L_3]$ coordination prism clearly shows the frontal mode for Cu_6 bound by three semirigid ligands. The two triangle facets of the prism are composed of two Cu_3 trimers featuring essentially planar nine-membered Cu_3N_6 rings with two-coordinate Cu^I sites, whereas the three edges perpendicular to

[a] G.-F. Gao,[+] M. Li,[+] S.-Z. Zhan, Z. Lv, Prof. G.-h. Chen, Prof. D. Li
Department of Chemistry, Shantou University
Guangdong 515063 (P.R. China)
Fax: (+86) 754-2902767
E-mail: dli@stu.edu.cn

[+] These authors contributed equally to this work.

Supporting information for this article is available on the WWW under http://dx.doi.org/10.1002/chem.201100081.

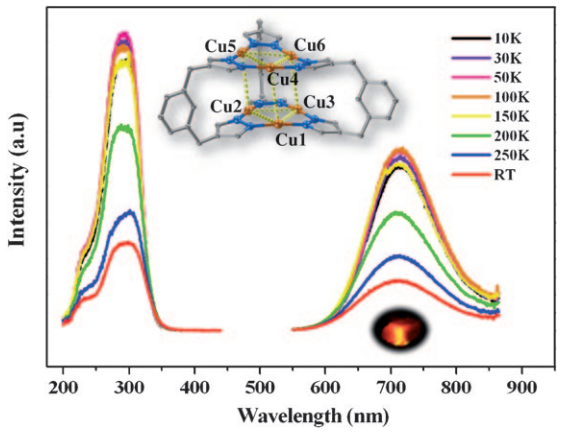

Figure 2. The crystal structure of the $[Cu_6L_3]$ coordination prism along with the temperature-dependent excitation and emission spectra. The crystal structure was measured at room temperature (298 K). Color codes: orange Cu, blue N, and gray C. The 3,5-dimethyl substituents of the pyrazolate rings as well as all H atoms of the ligands are omitted for clarity. The golden dashed lines depict the intra- and intertrimeric Cu^I–Cu^I interactions that form a prism configuration. Intratrimeric distances: Cu1–Cu2 3.174, Cu1–Cu3 3.217, Cu2–Cu3 3.203, Cu4–Cu5 3.195, Cu4–Cu6 3.212, and Cu5–Cu6 3.199 Å; intertrimeric distances: Cu1–Cu4 3.868, Cu2–Cu5 3.946, and Cu3–Cu6 3.696 Å. The crystalline sample of $[Cu_6L_3]$ shows intense red photoluminescence (as shown in the inserted picture below the emission spectra) with an emission band at $\lambda_{em}=716$ nm at room temperature, and an excitation band at $\lambda_{ex}=290$ nm. Upon lowering the temperature, both the intensity of the excitation and emission increased significantly, but no luminescent thermochromism was recorded.

these triangle facets consist of xylylene groups. The structure is slightly distorted from the ideal equilateral triangular prism configuration and hence crystallizes in the monoclinic $P2_1/c$ space group with an entire $[Cu_6L_3]$ molecule as the asymmetric unit (see Section 2 of the Supporting Information for additional structural illustrations). The intertrimeric Cu^I–Cu^I distances of 3.696, 3.868, and 3.946 Å (298 K), respectively, are generally longer than those measured in Cu_6, which exhibits eclipsed and staggered modes or a combination of the two (see Section 3 of the Supporting Information). Note that there are three Cu^I–Cu^I contacts herein, whereas only one or two Cu^I–Cu^I contacts exist in previous documentation.[7–12]

Three aspects of structural uniqueness of this coordination prism should be highlighted: 1) Compared with other heavier coinage metals (Ag^I and Au^I), the selection of the smaller and lighter Cu^I, with which relativistic effects are expected to be much less important,[13] lessens the complications when discussing the origin of the metallophilicity. 2) The length of the xylylene linker of ≈4.0 Å is much longer than the Cu–Cu van der Waals radii sum of 2.8 Å, significantly weakening intertrimeric Cu^I–Cu^I interactions at the ground state (S_0), but it is reasonable to speculate that the Cu_6 centers may interact strongly at the triplet excited state (T_1) and cause low-energy visible emissions. 3) The prism configuration allows geometrical confinement (even at T_1), where the above-mentioned parameters of l and α (Figure 1) are completely restricted and the variation of d is partially restricted due to the flexibility of methylene in the linker, warranting the unprecedented presence of the frontal mode of Cu_6.

Usually the emissive bands of Cu_3-based compounds range from 540 to 660 nm (see Section 3 of the Supporting Information) with microsecond lifetimes.[7–11] According to the extensive spectroscopic investigations by Che and coworkers,[14,15] these low-energy and long-lived emissions are attributed to phosphorescent, triplet, metal–metal-bonded, excited states (^{3}MM), whereas the excitations are singlet ligand-to-metal–metal charge transfers (^{1}LMMCT), which involve Cu^I 3dσ*→4pσ transitions, implying a bonding nature of the Cu^I–Cu^I interactions. In this $[Cu_6L_3]$ coordination prism, albeit the intertrimeric Cu^I–Cu^I distances are too long for ground-state bonding according to the crystal structure data, some interesting luminescent behaviors with similar unstructured, but also unique, profiles, are observed (Figure 2). The excitation spectra at a very short wavelength ($\lambda_{ex}=290$ nm) is required to generate the very long-wavelength emission spectra ($\lambda_{em}=716$ nm), showing very intense red emission with an obvious redshift compared with previously reported results.

This lowest-energy excited state ($\lambda_{em}=716$ nm, compared with 542 nm for the unassisted oligomeric Cu_3 dimer and 598 nm for the polymeric Cu_3-based frameworks)[11] would not be possible without the existence of the geometrical confinement and the presence of the frontal mode. Given that the excitation wavelengths are similar ($\lambda_{ex}=290$ nm, compared with 305 nm for the Cu_3-based oligomer and polymer),[11] we speculate that this lower-energy T_1 state is supported by the unprecedented three Cu^I–Cu^I interactions confined in the coordination prism, compared with one or two for other Cu_3 compounds. This geometrical confinement also enables the high activation energy needed for the internal conversion to a higher-energy T_1 state, and thus, there is only one possible emissive T_1 state for the coordination prism; this explains why the emission spectra only vary in intensity with different temperatures, whereas in other Cu_3-based compounds the phenomenon of luminescence thermochromism is usually observed.[7–9] Also, the temperature-dependent lifetimes of the $[Cu_6L_3]$ emission, ranging from 18.84 ± 0.04 to 24.66 ± 0.03 μs (see Section 4 of the Supporting Information), are consistent with the microsecond scale of phosphorescence. The colossal Stokes' shift (about 23470 cm^{-1}!) indicates that the excited states may experience huge distortion; this will be discussed below.

Other than the spectroscopic evidence mentioned above, from the structural point of view, the two Cu_3 triangles show a slight deviation from the planarity defined by the three edges, that is, the xylylene linkers of the prism with a length of ≈4.0 Å. Clearly the two Cu_3 triangles are attracted to each other, resulting in concave triangle facets compared with the planar triangle facets of an ideal prism. To assess the existence of such a metallophilic attraction, the crystal structure of $[Cu_6L_3]$ was measured at a cryogenic temperature. Accordingly, the three intertrimeric Cu^I–Cu^I separations are shorten by 0.1 Å, from 3.696, 3.868, and 3.946 Å

(average 3.837 Å, 298 K) to 3.556, 3.804, and 3.848 Å (average 3.736 Å, 143 K), respectively, implying enhancement of such an attraction at lower temperatures. But this trend is not reflected in the temperature-dependent luminescent spectra (Figure 2), and some previous works also showed that genuine ligand-unassisted cuprophilic attraction is not relevant to very short Cu^I–Cu^I distances.[16,17] In fact, it is questionable whether the compression of the Cu^I–Cu^I distances is due to the constraints of the bridging ligands or to genuine metal–metal interactions. A literature survey (see Section 3 of the Supporting Information) shows that the face value of Cu^I–Cu^I distances (related to the radii sum of 2.8 Å) is an unreliable criterion for assessing metallophilicity in the Cu_3 family.

Instead, energetic considerations by calculating the overall stabilization can provide more convincing evidence of metallophilicity. Theoretical treatments by Schwerdtfeger et al.[18] estimated that the pure cuprophilic bonding is in the range of 3.5–4 kcal mol^{-1} for the ligand-unassisted dimeric model that contains only one Cu^I–Cu^I contact, and for the unassisted Cu_3 dimer, with chair conformation and in which multiple Cu^I–Cu^I contacts exist, the intertrimeric cuprophilic stabilization at the S_0 state is calculated to be up to 18.1 kcal mol^{-1}.[10] Herein, we calculate the overall metallophilic stabilization for $[Cu_6L_3]$ (see Figure S6 in Section 5 of the Supporting Information for calculation details), resulting in a value of 19.74 kcal mol^{-1}, which is larger than in the above-mentioned reports. Despite the much longer intertrimeric Cu^I–Cu^I separation (3.837 Å on average) of $[Cu_6L_3]$ than those of the analogous Cu_3-based oligomer (2.954 Å) and polymer (3.331 Å),[11] the larger stabilization energy indicates enhanced cuprophilicity within the coordination prism. The three Cu^I–Cu^I contacts, which exist only in the frontal mode of the coordination prism, entail this enhanced metal–metal bonding, also manifested by the above-discussed structural and spectroscopic uniqueness.

The theoretical origin of the metallophilicity was interpreted as hybridization of *n*d orbitals with $(n+1)$s and $(n+1)$p orbitals[4] or as correlation effects strengthened by relativistic effects,[5] as introduced above. The key point of this contention is whether electronic transitions that form metal–metal bonds are involved. Early DFT calculations[6] disaffirmed this hypothesis, but recent time-dependent DFT (TDDFT) analysis performed by Cundari and co-workers,[10] who considered both the S_0 and T_1 states of cyclic, trinuclear, coinage metal pyrazolates, clearly showed HOMO–LUMO, intertrimeric, electron density transitions between the frontier orbitals of S_0 and T_1. The intriguing luminescent behaviors presented herein and for other members of the Cu_3 family[7–9] also imply a metal–metal bonding character.

Herein, we utilize TDDFT calculations to analyze the frontier orbitals of the optimized S_0 and T_1 states of $[Cu_6L_3]$. As shown in Figure 3, at the HOMO of S_0, the electron density is highly distributed on the ligands and metal–ligand coordinative bonds, whereas at the LUMO of S_0, the electron density is primarily located around the Cu atoms, showing delocalized, intertrimeric, Cu^I–Cu^I bonding across multiple

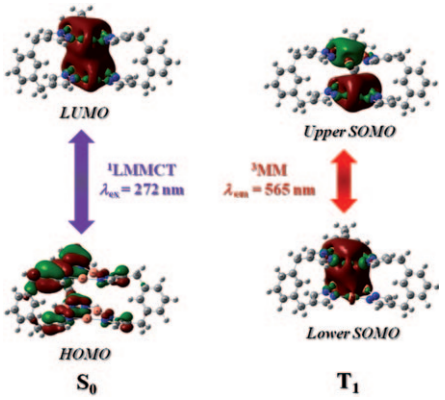

Figure 3. Frontier-orbital contours of the TDDFT-optimized S_0 and T_1 states of $[Cu_6L_3]$, showing the HOMO–LUMO band gap of S_0 and the lower–upper SOMOs band gap of T_1, assigned as excitation and emission bands, respectively. The geometrical optimization is based on the crystallographic data of $[Cu_6L_3]$. To simplify the calculation, the 3,5-dimethyl substituents of the pyrazolate rings were replaced by hydrogen atoms. The atomic labels and positions are consistent with the crystal structure shown in Figure 2. Color codes: orange Cu, blue N, gray C and H; the electron density is shown in red and green. The optimized Cu^I–Cu^I separations are given below. For S_0, intratrimeric distances: Cu1–Cu2 3.227, Cu1–Cu3 3.208, Cu2–Cu3 3.247, Cu4–Cu5 3.227, Cu4–Cu6 3.217, and Cu5–Cu6 3.239 Å; intertrimeric distances: Cu1–Cu4 4.165, Cu2–Cu5 4.183, and Cu3–Cu6 3.982 Å. For T_1, intratrimeric distances: Cu1–Cu2 3.219, Cu1–Cu3 3.230, Cu2–Cu3 3.231, Cu4–Cu5 2.594, Cu4–Cu6 2.554, and Cu5–Cu6 3.047 Å; intertrimeric distances: Cu1–Cu4 3.407, Cu2–Cu5 3.584, and Cu3–Cu6 3.555 Å.

Cu^I centers. This HOMO–LUMO band-gap energy is assigned as the excitation band of ^{1}LMMCT and calculated to appear at $\lambda_{ex}=272$ nm, which is close to the experimental value of 290 nm. For the phosphorescent T_1 state, the upper singly occupied molecular orbital (SOMO) shows increased intertrimeric bonding compared with the singlet LUMO, whereas the lower SOMO populated with intratrimeric density indicates the disconnection of the intertrimeric Cu^I–Cu^I bonding. The emission band of the ^{3}MM state is attributed to the upper-to-lower SOMOs band-gap energy of T_1, with a calculated emission band at $\lambda_{em}=565$ nm (experimental $\lambda_{em}=716$ nm). Compared with previous modeling of the photophysics of Cu_3 systems (see Table S6 in Section 5 of the Supporting Information), this result is acceptable. The theoretical assignments of the luminescent spectra are consistent with the above-discussed experimental data.

Further structural clues are carefully examined to rationalize the unprecedented geometry of the coordination prism and the unique photophysical behaviors. The above-mentioned geometrical optimization (Figure 3) gives rise to the intertrimeric Cu^I–Cu^I distances (3.982, 4.165, 4.183; average 4.110 Å) at S_0; these are slightly longer than the experimental values (3.696, 3.868, 3.946; average 3.837 Å), whereas at T_1 the calculated values (3.555, 3.407, 3.584; average 3.515 Å) are shorten by 0.595 Å on average (see Figure S5 and Table S5 in Section 5 of the Supporting Information for details). This result is experimentally supported by a recent study by Coppens and co-workers,[19] who developed the technique of time-resolved single-crystal X-ray diffraction

and determined the excited-state structure of an unassisted Cu_3 dimer to show that one of the Cu^I–Cu^I distances therein was reduced by 0.56 Å from 4.018 Å at S_0 to 3.461 Å at T_1. The drastic distortion in the geometry of the emissive excited state of $[Cu_6L_3]$ corresponds to the above-mentioned colossal Stokes' shift of $\approx 23470\ cm^{-1}$.

With such a significant geometrical adjustment, the pseudo-D_{3h} symmetry (equilateral triangle) at S_0 of the $[Cu_6L_3]$ coordination prism is reduced to pseudo-C_{2v} symmetry (isosceles triangle) at T_1. Notably, one site of the six Cu^I atoms in $[Cu_6L_3]$, namely Cu4, is mainly responsible for this drastic distortion; the distance between Cu4 and Cu1 is reduced by 0.758 Å from 4.165 Å at S_0 to 3.407 Å at T_1 (both calculated). Such intense contraction operated by the enhanced Cu^I–Cu^I bonding at the excited state even overwhelms the Cu–N coordinative bonds. As shown in Figure 4, the linear geometry of two-coordinate Cu^I is destructed and the Cu–N distances are significantly elongated by ≈ 0.2 Å. Such an unusual phenomenon is referred to as photoinduced Jahn–Teller distortion,[10,20–22] which describes the drastic geometrical adjustment in the T_1 states of d blocks and the corresponding spectroscopic uniqueness, such as huge Stokes' shifts and phosphorescent emissions.

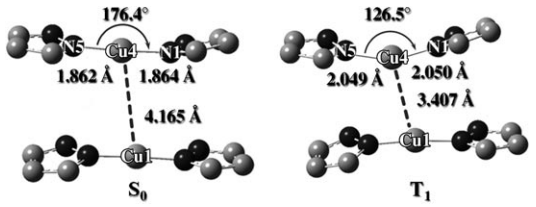

Figure 4. Partial structural views of the optimized bonding environment of Cu4 in $[Cu_6L_3]$, illustrating the drastic geometrical distortion from the S_0 to the T_1 state. Only Cu4 and Cu1 along with the corresponding coordinated pyrazolate components are depicted here. The $Cu1^I$–$Cu4^I$ bonds are shown in dashed lines and the N5-Cu4-N1 bond lengths and angles are marked. From the S_0 to the T_1 state, the $Cu1^I$–$Cu4^I$ separation is dramatically shorten by 0.758 Å from 4.165 to 3.407 Å, whereas the Cu–N bonds are elongated by 0.19 Å from ≈ 1.86 to 2.05 Å, and the N5-Cu4-N1 angle is reduced by up to 49.9° from 176.4 to 126.5°.

A logical explanation for such a huge distortion is that the lowest-energy excited state of $[Cu_6L_3]$ involves electronic transitions from filled 3d antibonding orbitals to vacant bonding orbitals arising from 4s and 4p subshells. This hypothesis is testified herein by examining the composition of the frontier orbitals of $[Cu_6L_3]$ deduced from the above TDDFT calculations. As shown in Table S7 in the Supporting Information, at the site of Cu4, the located electron density accounts for up to 42.8% (of which 31.2% arise from the s subshell and 10.6% from the p subshell) of the overall population in the HOMO of T_1. In this case, it is reasonable that at the triplet excited state of $[Cu_6L_3]$, the existence of metallophilicity significantly weakens the coordinating ability of Cu4, because the 4s and 4p subshells of Cu4 are partially occupied by the promoted 3d electrons. This means that one Cu^I–Cu^I bond can overwhelm the related Cu–N coordinative bonds. This grand orbital mixing is responsible for the decrease of the SOMOs band gap in the phosphorescent state, thus leading to the redshift of the low-energy and long-lived emission of the coordination prism.

Taken together, we have reached three conclusions in this research: 1) In this $[Cu_6L_3]$ coordination prism, the occurrence of enhanced cuprophilicity is unambiguously evidenced by structural, spectroscopic, and computational investigations. 2) The phosphorescent emission assignment and frontier-orbital analysis suggest that the intertrimeric Cu^I–Cu^I contacts within this coordination prism involve natural electronic transitions. 3) It is reasonable to speculate that the reason for this Cu^I–Cu^I bonding is orbital hybridization (3d, 4s and 4p), which is supported by examining the composition of the frontier orbitals of $[Cu_6L_3]$, especially for the Cu4 site with significant photoinduced Jahn–Teller distortion. This newly designed coordination prism that exhibits an unprecedented stacking mode represents a unique case for assessing the existence and the nature of metallophilicity within a confined space.[23,26] Further, this research suggests that there should be no generalization for the nature of metallophilicity—in this case evident metallophilicity accompanied by electron transitions seems warranted, but in other cases the effects of bridging ligands and electrostatic interactions may obscure any genuine metallophilicity. Since metallophilicity is widely considered by theoretical chemists as a type of van der Waals force, it is highly recommended that further computational assessment is performed by taking advantage of the recently developed model of DFT with long-range corrections.[24]

Experimental Section

Synthesis of $[Cu_6L_3]$: A mixture of Cu_2O (0.0288 g, 2.0 mmol), HL (0.0147 g, 1.0 mmol), *n*-hexane (4.0 mL), and acetonitrile (4.0 mL) was stirred for 15 min in air. It was then transferred and sealed in a 12 mL Teflon-lined reactor, which was heated in an oven at 140 °C for 72 h and then cooled to room temperature at a rate of 3 °C 0.5 h^{-1}. Yellowish block crystals of $[Cu_6L_3]$ were obtained as the major product (see Section 1 of the Supporting Information for additional synthetic details)

Crystallographic study of $[Cu_6L_3]$: Data collection was performed on a Bruker Smart Apex CCD diffractometer ($Mo_{K\alpha}$, $\lambda = 0.71073$ Å) by using SMART (Bruker AXS, Madison, WI, USA, 1997) at 298 and 143 K. Reflection intensities were integrated with the SAINT software and absorption correction was applied semiempirically (Bruker AXS, Madison, WI, USA, 1997). The structures were solved by direct methods and refined by full-matrix least-squares refinements based on F^2. Anisotropic thermal parameters were applied to all non-hydrogen atoms. The hydrogen atoms were generated geometrically (C–H = 0.960 Å). The crystallographic calculations were conducted with the SHELXL-97 programs. Crystal data for $[Cu_6L_3]$: 298 K; $Cu_6C_{54}H_{60}N_{12}$; $M_r = 1258.38$; monoclinic; space group $P2_1/c$; $a = 20.0870(16)$, $b = 29.696(2)$, $c = 9.2062(7)$ Å; $\beta = 94.919(2)°$; $V = 5471.2(7)$ Å^3; $Z = 4$; $\rho_{calcd} = 1.528$ g cm^{-3}; $\mu = 2.338$ mm^{-1}; $F(000) = 2568$; 31535 reflections collected; 9579 unique reflections ($R_{int} = 0.0461$); $R_1 = 0.0932$ and $wR_2 = 0.1371$ for all data; $R_1 = 0.0461$ and $wR_2 = 0.1026$ for data with $I > 2\sigma(I)$: 143 K; $Cu_6C_{54}H_{60}N_{12}$; $M_r = 1258.38$; monoclinic; space group $P2_1/c$; $a = 20.0147(12)$, $b = 29.5576(18)$, $c = 9.0406(6)$ Å; $\beta = 95.3590(10)°$; $V = 5324.9(6)$ Å^3; $Z = 4$; $\rho_{calcd} = 1.570$ g cm^{-3}; $\mu = 2.402$ mm^{-1}; $F(000) = 2568$; 37561 reflections collected; 9351 unique reflections ($R_{int} = 0.0379$); $R_1 = 0.0566$ and $wR_2 = 0.1135$ for all data, $R_1 =$

0.0409 and $wR_2 = 0.0963$ for data with $I > 2\sigma(I)$. CCDC-784867 (298 K) and 784868 (143 K) contain the supplementary crystallographic data for this paper. These data can be obtained free of charge from The Cambridge Crystallographic Data Centre via www.ccdc.cam.ac.uk/data_request/cif. See Section 1 of in the Supporting Information for additional crystallographic details.

Spectroscopic study of $[Cu_6L_3]$: Solid-state luminescence spectra were acquired with an Edinburg FLS920 fluorescence spectrometer equipped with a continuous Xe 900 Xenon lamp. Lifetime data were acquired with a single-photon-counting spectrometer with a hydrogen-filled pulse lamp as the excitation source. For low-temperature measurements, the samples were mounted on a closed-cycle cryostat (10–350 K, DE 202, Advanced Research Systems), interfaced with a liquid helium tank. See Section 4 of in the Supporting Information for additional luminescent measurement details.

Computational study of $[Cu_6L_3]$: Theoretical calculations were performed with the Gaussian03 program package.[25] The optimized geometries of the local minima were obtained at the DFT/B3LYP level of theory. The 6–31G(d) basis set was used for C, N and H elements, whereas the Lanl2dz effective core potential (ECP) basis set was used for Cu elements. The counterpoise method was used to eliminate basis-set superposition errors (BSSEs). See Section 5 of in the Supporting Information for additional theoretical calculation details.

Acknowledgements

This work is financially supported by the National Natural Science Foundation for Distinguished Young Scholars of China (20825102) and the National Natural Science Foundation of China (20571050 and 20771072).

Keywords: cage compounds · Cu–Cu interactions · density functional calculations · luminescence · metallophilicity

[1] M. Jansen, *Angew. Chem.* **1987**, *99*, 1136–1149; *Angew. Chem. Int. Ed. Engl.* **1987**, *26*, 1098–1110.
[2] H. Schmidbaur, A. Schier, *Chem. Soc. Rev.* **2008**, *37*, 1931–1951.
[3] J. M. Zuo, M. Kim, M. O'Keeffe, J. C. H. Spence, *Nature* **1999**, *401*, 49–52.
[4] K. M. Merz, Jr., R. Hoffmann, *Inorg. Chem.* **1988**, *27*, 2120–2127.
[5] P. Pyykkö, *Chem. Rev.* **1997**, *97*, 597–636.
[6] F. A. Cotton, X. Feng, D. J. Timmons, *Inorg. Chem.* **1998**, *37*, 4066–4069.
[7] H. V. R. Dias, H. V. K. Diyabalanage, M. A. Rawashdeh-Omary, M. A. Franzman, M. A. Omary, *J. Am. Chem. Soc.* **2003**, *125*, 12072–12073.
[8] H. V. R. Dias, H. V. K. Diyabalanage, M. G. Eldabaja, O. Elbjeirami, M. A. Rawashdeh-Omary, M. A. Omary, *J. Am. Chem. Soc.* **2005**, *127*, 7489–7501.
[9] M. A. Omary, M. A. Rawashdeh-Omary, M. W. A. Gonser, O. Elbjeirami, T. Grimes, T. R. Cundari, *Inorg. Chem.* **2005**, *44*, 8200–8210.
[10] T. Grimes, M. A. Omary, H. V. R. Dias, T. R. Cundari, *J. Phys. Chem. A* **2006**, *110*, 5823–5830.
[11] J. He, Y.-G. Yin, T. Wu, D. Li, X.-C. Huang, *Chem. Commun.* **2006**, 2845–2847.
[12] J.-P. Zhang, S. Kitagawa, *J. Am. Chem. Soc.* **2008**, *130*, 907–917.
[13] M. A. Carvajal, S. Alvarez, J. J. Novoa, *Chem. Eur. J.* **2004**, *10*, 2117–2132.
[14] C.-M. Che, Z. Mao, V. M. Miskowski, M.-C. Tse, C.-K. Chan, K.-K. Cheung, D. L. Phillips, K.-H. Leung, *Angew. Chem.* **2000**, *112*, 4250–4254; *Angew. Chem. Int. Ed.* **2000**, *39*, 4084–4088.
[15] C.-M. Che, S.-W. Lai, *Coord. Chem. Rev.* **2005**, *249*, 1296–1309.
[16] R. D. Köhn, G. Seifert, Z. Pan, M. F. Mahon, G. Kociok-Köhn, *Angew. Chem.* **2003**, *115*, 818–820; *Angew. Chem. Int. Ed.* **2003**, *42*, 793–796.
[17] K. Singh, J. R. Long, P. Stavropoulos, *J. Am. Chem. Soc.* **1997**, *119*, 2942–2943; *Inorg. Chem.* **1998**, *37*, 1073–1079.
[18] H. L. Hermann, G. Boche, P. Schwerdtfeger, *Chem. Eur. J.* **2001**, *7*, 5333–5342.
[19] I. I. Vorontsov, A. Yu. Kovalevsky, Y.-S. Chen, T. Graber, M. Gembicky, I. V. Novozhilova, M. A. Omary, P. Coppens, *Phys. Rev. Lett.* **2005**, *94*, 193003.
[20] K. A. Barakat, T. R. Cundari, M. A. Omary, *J. Am. Chem. Soc.* **2003**, *125*, 14228–14229.
[21] V. R. Bojan, Fernández, E. J. A. Laguna, J. M. López-de-Luzuriaga, M. Monge, M. E. Olmos, C. Silvestru, *J. Am. Chem. Soc.* **2005**, *127*, 11564–11565.
[22] M. Iwamura, S. Takeuchi, T. Tahara, *J. Am. Chem. Soc.* **2007**, *129*, 5248–5256.
[23] T. Osuga, T. Murase, K. Ono, Y. Yamauchi, M. Fujita, *J. Am. Chem. Soc.* **2010**, *132*, 15553–15555. This most recent paper published during the submission of this work shows a gold(I)-pyrazolate-trimer array with a frontal mode, which is confined in a host coordination cage, showing the importance of such an unprecedented stacking mode in this system of complexes.
[24] J. A. Alonso, A. Mañanes, *Theor. Chem. Acc.* **2006**, *117*, 467–472.
[25] Gaussian 03, Revision C.02, M. J. Frisch, G. W. Trucks, H. B. Schlegel, G. E. Scuseria, M. A. Robb, J. R. Cheeseman, J. A. Montgomery, Jr., T. Vreven, K. N. Kudin, J. C. Burant, J. M. Millam, S. S. Iyengar, J. Tomasi, V. Barone, B. Mennucci, M. Cossi, G. Scalmani, N. Rega, G. A. Petersson, H. Nakatsuji, M. Hada, M. Ehara, K. Toyota, R. Fukuda, J. Hasegawa, M. Ishida, T. Nakajima, Y. Honda, O. Kitao, H. Nakai, M. Klene, X. Li, J. E. Knox, H. P. Hratchian, J. B. Cross, V. Bakken, C. Adamo, J. Jaramillo, R. Gomperts, R. E. Stratmann, O. Yazyev, A. J. Austin, R. Cammi, C. Pomelli, J. W. Ochterski, P. Y. Ayala, K. Morokuma, G. A. Voth, P. Salvador, J. J. Dannenberg, V. G. Zakrzewski, S. Dapprich, A. D. Daniels, M. C. Strain, O. Farkas, D. K. Malick, A. D. Rabuck, K. Raghavachari, J. B. Foresman, J. V. Ortiz, Q. Cui, A. G. Baboul, S. Clifford, J. Cioslowski, B. B. Stefanov, G. Liu, A. Liashenko, P. Piskorz, I. Komaromi, R. L. Martin, D. J. Fox, T. Keith, M. A. Al-Laham, C. Y. Peng, A. Nanayakkara, M. Challacombe, P. M. W. Gill, B. Johnson, W. Chen, M. W. Wong, C. Gonzalez, J. A. Pople, Gaussian, Inc., Wallingford CT, **2004**.
[26] **Note added in proof (7.3.2011)**: During the proof of the this work a paper was published that described the synthesis, structure, and luminescence of a Cu6 coordination cage with a staggered mode (T. Jozak, Y. Sun, Y. Schmitt, S. Lebedkin, M. Kappes, W. R. Thiel, *Chem. Eur. J.* **2011**, *17*, 3384–3389).

Received: January 9, 2011
Published online: March 11, 2011

